Membrane Channel Forming Polypeptides. Molecular Conformation and Mitochondrial Uncoupling Activity of Antiamoebin, an α-Aminoisobutyric Acid Containing Peptide[†]

Manoj K. Das, S. Raghothama, and P. Balaram*

Molecular Biophysics Unit and Sophisticated Instruments Facility, Indian Institute of Science, Bangalore 560 012, India

Received March 20, 1986; Revised Manuscript Received July 14, 1986

ABSTRACT: The conformations of the 16-residue fungal peptide antiamoebin I (Ac-Phe-Aib-Aib-Aib-D-Iva-Gly-Leu-Aib-Aib-Hyp-Gln-D-Iva-Hyp-Aib-Pro-Phol) have been investigated in dimethyl sulfoxide solution by one- and two-dimensional NMR techniques. A substantial number of resonances in the 270-MHz ^{1}H NMR spectrum have been assigned. Intramolecularly hydrogen-bonded (solvent inaccessible) NH groups have been identified by determining solvent and temperature dependence of NH chemical shifts and rates of hydrogen–deuterium exchange. Ten backbone NH groups are inaccessible to solvent, while three NH groups assigned to the Phe(1), Aib(2), and Aib(8) residues are exposed to solvent. Interresidue nuclear Overhauser effects are consistent with ψ values of $\sim 120 \pm 30°$ for Phe(1) and Leu(7). The NMR results, together with the stereochemical constraints imposed by the presence of α-aminoisobutyryl, isovalyl, prolyl, and 4-hydroxyprolyl residues, favor a highly ordered structure. Two backbone conformations consistent with the data are considered. Antiamoebin is shown to be an effective uncoupler of oxidative phosphorylation in rat liver mitochondria, providing evidence for its membrane-modifying activity.

Membrane-modifying peptides of fungal origin, which are rich in α-aminoisobutyric acid (Aib), have been the focus of several recent investigations (Mathew & Balaram, 1983a; Jung et al., 1981). Representative sequences are listed in Figure 1. Alamethicin, a 20-residue polypeptide, which forms voltage-gated channels across lipid bilayer membranes (Mueller & Rudin, 1967; Boheim & Kolb, 1978; Hall et al., 1984), is the most widely studied member of this class of peptides (Mathew & Balaram, 1983; Jung et al., 1981; Fox & Richards, 1982; Hall et al., 1984). The Aib-containing fungal peptides are characterized by a remarkable microheterogeneity of the natural products and occur as complex mixtures of closely related sequence analogues (Balasubramanian et al., 1981; Rinehart et al., 1981; Brückner et al., 1984; Brückner & Przybylski, 1984; Przybylski et al., 1984). Acetylation of the amino-terminal and the presence of a C-terminal β-amino alcohol are common features of these sequences. The Aib-containing natural peptides may be broadly grouped into two classes: (i) the "long" sequences that contain 18–20 residues and lack hydroxyproline (Hyp), as exemplified by the alamethicins (Pandey et al., 1977a), suzukacillins (Katz et al., 1985), trichotoxins (Przybylski et al., 1984), hypelcins (Fujita et al., 1984), paracelsins (Przybylski et al., 1984), and trichorzianines (Bodo et al., 1985) and (ii) the "short" sequences that contain 15–16 residues and possess hydroxylated residues, particularly Hyp, as exemplified by the emerimicins (Pandey et al., 1977b), zervamicins (Rinehart et al., 1981), and antiamoebins (Pandey et al., 1977c).

While alamethicin, suzukacillin, and trichotoxin have been shown to form stable conductance states in artificial lipid bilayers (Boheim et al., 1976; Boheim et al., 1978; Hall et al., 1984), definitive data have not been reported for the shorter peptides. However, references to the pore-forming activities of the antiamoebins, zervamicins, and emerimicins have appeared in the literature [see footnotes in Pandey et al.

(1977b,c) and Rinehart et al. (1981)]. There are no reports on detailed structural studies on the shorter peptides. Conformational analysis of the short sequences assumes importance in view of the presence of as many as three Pro or Hyp residues in the C-terminal segments of zervamicins, emerimicins, and antiamoebins. These should interrupt intramolecular hydrogen bonding and may result in structures distinctly different from those inferred for the alamethicin C-terminal (Fox & Richards, 1982; Mathew & Balaram, 1983a; Bosch et al., 1985a; Banerjee et al., 1983). We describe in this paper an NMR study of antiamoebin I that permits the development of secondary structural models for this sequence. We also establish the membrane–modifying activity of this peptide by demonstrating its effectiveness as a mitochondrial uncoupler.

MATERIALS AND METHODS

Antiamoebin, a fungal peptide produced by the strains *Emericellopsis poonensis* Thirum., *Emericellopsis synnematicola* Mathur and Thirum., and *Cephalosporium pimprina* Thirum., was the kind gift of Dr. N. Narasimhachari, Medical College of Virginia, Virginia Commonwealth University, and was originally isolated at Hindustan Antibiotics, Pune, India, as described earlier (Thirumalachar, 1968). Reverse-phase high-performance liquid chromatography (HPLC) analysis of the peptide was carried out on a Lichrosorb RP-18 column (4 × 250 mm, 10-μm particle size) with gradient elution (65–85% MeOH–H$_2$O in 20 min, 85–95% MeOH–H$_2$O in 5 min, flow 0.8 mL min^{-1}, detection 226 nm) on an LKB HPLC system. Purification of the peptide was effected by repetitive injections and collection of fractions using a Superrac fraction collector. For NMR studies, the peptide was used without HPLC purification (see Results and Discussion).

^{1}H NMR spectra were recorded on a Bruker WH-270 FT-NMR spectrometer, equipped with an Aspect 2000 computer at the Sophisticated Instruments Facility, Indian Institute of Science, Bangalore. For correlated spectroscopy (COSY) (Figure 4), 512 free induction decays (FIDs), each of 24 accumulations, with 1-s relaxation delay were collected. The

Alamethicin I : Ac-Aib-Pro-Aib-Ala-Aib-Ala-Gln-Aib-Val-Aib-Gly-Leu-Aib-Pro-Val-
Aib-Aib-Glu-Gln-Phol

Suzukacillin : Ac-Aib-Ala-Aib-Ala-Aib-Ala-Gln-Aib-Aib-Aib-Gly-Leu-Aib-Pro-Val-
Aib-Aib-Gln-Gln-Phol

Trichotoxin A-50 : Ac-Aib-Gly-Aib-Leu-Aib-Gln-Aib-Aib-Aib-Ala-Ala-Aib-Pro-Leu-Aib-
D-Iva-Gln-Valol

Zervamicin IIA : Ac-Trp-Ile-Gln-Aib-Ile-Thr-Aib-Leu-Aib-Hyp-Gln-Aib-Hyp-Aib-Pro-
Phol

Antiamoebin I : Ac-Phe-Aib-Aib-Aib-D-Iva-Gly-Leu-Aib-Aib-Hyp-Gln-D-Iva-Hyp-
Aib-Pro-Phol

FIGURE 1: Sequences of some Aib-containing membrane-modifying peptides. The sequences shown correspond to a single major component and are taken from the references mentioned in the text.

t_1 domain was zero filled to 1K, while 1K data points were collected in the t_2 domain resulting in a 1K × 1K data matrix. Phase-shifted sine bell window functions were applied prior to Fourier transformation on both domains. The spectral width in each dimension was 2500 Hz. Single channel detection with constant phase of pulses was used. In the difference nuclear Overhauser effect (NOE) experiments, the perturbed and normal spectra recorded sequentially (one on-resonance and one off-resonance) in different parts of the memory (8K of each) were obtained by low-power on-resonance saturation of a peak and by off-resonance shifting of the irradiation frequency, respectively. About 128 transients were accumulated with a relaxation delay of 3 s between transients to facilitate buildup of initial magnetization (Rao et al., 1983). Delineation of hydrogen-bonded NH groups was carried out as described earlier (Balaram, 1985; Kishore et al., 1985).

Peptide effects on respiration of rat liver mitochondria were monitored with a Hansatech oxygen electrode as described earlier (Das et al., 1985).

RESULTS AND DISCUSSION

Figure 2 shows an HPLC analysis of the sample of antiamoebin used in this study. A major component (∼80%) is observed with a retention time of ∼21 min. A significant second component (18%) is seen at ∼20 min, while at least three minor components (1–2%) are also discernible. Four pure fractions with retention times of 20.4, 21.4, 23.7, and 24.7 min have been isolated by HPLC separation and shown to correspond to closely related polypeptides. The microheterogeneity of natural antiamoebin has been noted earlier (Pandey et al., 1977c; Rinehart et al., 1979). Sequence analogues of the antiamoebin I sequence, where the replacements of Pro for Hyp(13), Aib for Iva(5), and Ala for Gly(6) occur, have been characterized by mass spectrometry (Pandey et al., 1978; Stroh et al., 1985). The 270-MHz ^{1}H NMR spectrum of the purified major component (retention time 21.7 min) was practically indistinguishable from that of unpurified antiamoebin. All NMR studies were therefore carried out without further purification of the antiamoebin sample. The 270-MHz ^{1}H NMR spectrum of antiamoebin in $(CD_3)_2SO$ is shown in Figure 3. The spectrum is fully consistent with the composition suggested for antiamoebin I (Figure 1, Pandey et al., 1977c). The amino acid analysis and ^{13}C NMR spectrum of the peptide provide further confirmation (data not shown). Antiamoebin is largely insoluble in water, sparingly soluble in chloroform, and appreciably soluble in dimethyl sulfoxide. Conformational studies were therefore carried out in $(CD_3)_2SO$.

Assignment of Resonances. Figure 4 shows the two-dimensional correlated spectrum (Aue et al., 1976; Wider et al., 1984) of antiamoebin in $(CD_3)_2SO$. The five expected connectivities between the NH and $C^{\alpha}H$ resonances [Phe(1),

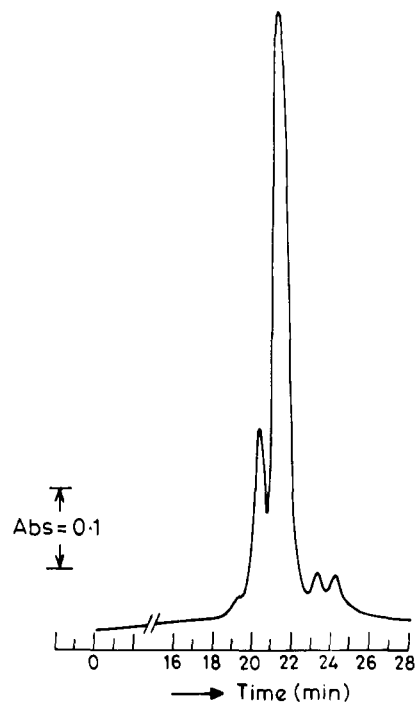FIGURE 2: HPLC profile for antiamoebin (1 mg of peptide in 20 μL of MeOH). Conditions are as described under Materials and Methods.

Gly(6), Leu(7), Gln(11), Phol(16)] are clearly seen. The Gly NH group is readily recognized by its triplet nature and its coupling to the resonance at δ 3.74 ($C^{\alpha}H_2$), which in turn displays no further connectivity. The Gln spin system is characterized by the $C^{\beta}H_2$ (δ 1.818)–$C^{\gamma}H_2$ (δ 2.187) connectivity, which permits identification of the Gln $C^{\alpha}H$ (δ 4.17) and NH (δ 7.90) resonances. The Phe and Phol residues have overlapping $C^{\beta}H$ resonances in the region δ 2.55–3.00. The Phol $C^{\alpha}H$ resonance is however observed at significantly higher field (δ 3.818) as compared to the Phe $C^{\alpha}H$ group (δ 4.340). A similar chemical shift has been reported for Phol $C^{\alpha}H$ in alamethicin (Martin & Williams, 1976). This resonance is also unambiguously identified by its connectivity to resonances at δ 3.2–3.5 (Phol $C^{\beta}H_2$), which in turn are coupled to a triplet OH resonance at δ 4.62. This hydroxyl proton resonance disappears on addition of D_2O. The entire Leu spin system cannot be unambiguously traced in the COSY spectrum due to overlap of the $C^{\beta}H_2$ and $C^{\gamma}H$ resonances (Nagayama & Wüthrich 1981; Davoust et al., 1983). However, the assignments of the $C^{\alpha}H$ and NH protons are unequivocal, since all other residues with coupled $C^{\alpha}H$ and NH resonances have been identified. The Hyp $C^{\alpha}H$ and $C^{\gamma}H$ resonances were assigned by virtue of their common connectivities to the $C^{\beta}H_2$ resonances, while the $C^{\gamma}H$ protons were also coupled to the hydroxyl resonances at δ 5.18. The assignments are indicated in Figure 3, and the proton chemical shifts of unambiguously identified residues are summarized in Table I. An unambiguous assignment of the various singlet resonances to specific Aib/Iva residues is not possible at present. The singlet NH resonances at δ 6.78 and 7.29 correspond to the Gln carboxamide side-chain protons. A small geminal coupling between these protons is not detected in Figure 3, but is clearly observed as an off-diagonal cross peak in the COSY spectrum (Figure 4). In the low-field region, 15 NH resonances can be identified, due to 13 backbone and 2 side-chain NH groups. Resonances are labeled S_n, D_n, and T_n, where S, D, and T denote singlets, doublets, and triplets, respectively, while the subscript n indicates the order of appearance from low field in $(CD_3)_2SO$ (Figure 5).

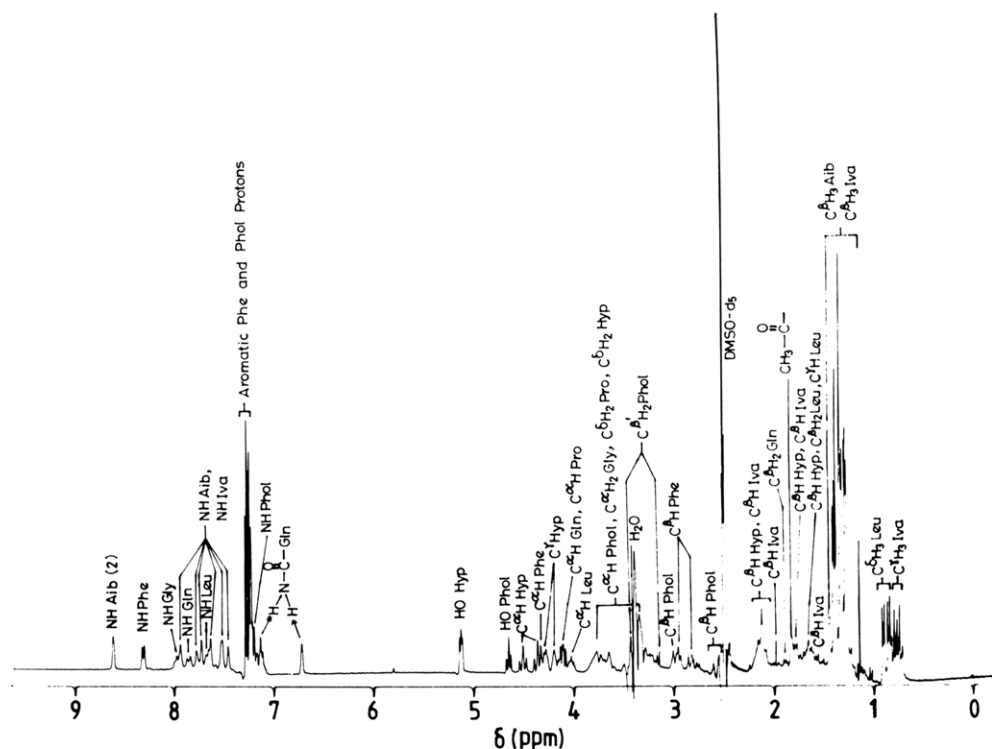FIGURE 3: 270-MHz ^{1}H NMR spectrum of antiamoebin in dimethyl sulfoxide-d_6, $(CD_3)_2SO$ (20 mg mL^{-1}). Assignments indicated were derived from COSY experiments (see Figure 4).

Table I: Proton Chemical Shifts[a] for Specific Residues of Antiamoebin in $(CD_3)_2SO$

residue	chemical shifts, δ		
	NH	C$^\alpha$H	others
Phe(1)	8.32 (D$_2$)	4.33	2.95, 2.82 (C$^\beta$H)
			7.29–7.22 (aromatic protons)
Gly(6)	7.98 (T$_3$)	3.64	
Gln(11)	7.86 (D$_5$)	4.12	1.88 (C$^\beta$H$_2$)
			7.14, 6.73 (–CONH)
Leu(7)	7.67 (D$_8$)	4.03	1.65 (C$^\beta$H$_2$, C$^\gamma$H)
			0.90, 0.84 (C$^\delta$H$_3$)
Phol(16)	7.20 (D$_{13}$)	3.73	3.00, 2.56 (C$^\beta$H)
			3.43, 3.14 (C$^{\beta'}$H)
			4.66 (–OH)
			7.29–7.22 (aromatic protons)
Hyp(10, 13)[b]		4.51	5.13 (–OH), 4.28 (C$^\gamma$H)
			2.11, 1.77 (C$^\beta$H), 4.40 (C$^\alpha$H)
Hyp(10, 13)[b]		4.37	5.13 (–OH), 4.20 (C$^\gamma$H)
			2.11, 1.67 (C$^\beta$H), 4.54 (C$^\alpha$H)

[a] All Aib and Iva resonances cannot be assigned to specific residues in the sequence. The chemical shift values for these protons are therefore not tabulated. However, the Aib(2) NH and Aib(8) NH resonances have been identified by NOE connectivity to the preceding C$^\alpha$H resonance (see text and Table II for δ values). [b] The assignment of the Hyp spin systems to specific residues in the sequence is not possible at the present.

Table II: NMR Parameters[a] for Backbone NH Resonances in Antiamoebin

resonance	δ	dδ/dT (ppm/K)	resonance	δ	dδ/dT (ppm/K)
S$_1$	8.62	0.0065	D$_8$	7.71	0.0017
D$_2$	8.32	0.0052	S$_9$	7.63	0.0028
T$_3$	7.98	0.0024	S$_{10}$	7.54	0.0023
S$_4$	7.95	0.0015	S$_{11}$	7.53	0.0011
D$_5$	7.86	0.0017	S$_{12}$	7.48	0.0007
S$_6$	7.77	0.0049	D$_{13}$	7.17	0.0013
S$_7$	7.75	0.0022			

[a] δ values are reported at 294 K at a peptide concentration of 7.3 mM in $(CD_3)_2SO$ downfield from internal tetramethylsilane.

Delineation of Hydrogen-Bonded NH Groups. The possible involvement of NH groups in intramolecular hydrogen bonding was probed with three criteria (Kessler, 1982; Balaram, 1985; Wüthrich, 1976): (i) temperature dependence of NH chemical shifts, (ii) solvent dependence of NH chemical shifts in CDCl$_3$–$(CD_3)_2SO$ mixtures, and (iii) hydrogen–deuterium (H–D) exchange studies in $(CD_3)_2SO$–D$_2$O mixtures.

The temperature dependence of chemical shifts in $(CD_3)_2SO$ is linear for all the NH groups in antiamoebin (Figure 6). The chemical shifts (293 K) and temperature coefficients (dδ/dT) are summarized in Table II. Ten backbone resonances exhibit low dδ/dT values (<0.003 ppm/K) characteristic of solvent-shielded (intramolecularly hydrogen-bonded) NH groups. Three resonances [S$_1$, D$_2$ (Phe), and S$_6$] have high dδ/dT

values (>0.005 ppm/K) indicative of their exposure to solvent. Figure 7 shows the NH resonances at various time intervals after addition of D$_2$O (~10% v/v) to a $(CD_3)_2SO$ solution. Resonances S$_1$, D$_2$, and S$_6$ and one Gln side-chain proton (S$_{15}$) exchange relatively rapidly. S$_4$, D$_5$, and S$_{12}$ exhibit very slow exchange rates, while all the other NH resonances exchange appreciably slowly, indicative of their solvent-shielded nature. Representative spectra of antiamoebin in CDCl$_3$–$(CD_3)_2SO$ mixtures are illustrated in Figure 5. The solvent dependence of NH chemical shifts is summarized in Figure 8. An increase in the concentration of the strongly hydrogen-bond-accepting solvent, $(CD_3)_2SO$, results in significant downfield shifts of resonances S$_1$, D$_2$, and S$_6$ and the two Gln side-chain NH resonances. (Note that the chemical shift scale used for the side-chain NH resonances in Figure 8 is compressed relative to that used for the backbone NH protons.)

The results summarized above establish that resonances S$_1$, D$_2$, and S$_6$ may be assigned to fully solvent exposed NH groups. The behavior of the remaining 10 backbone NH resonances is characteristic of solvent-shielded/intramolecularly hydrogen-bonded NH groups.

Nuclear Overhauser Effects. Nuclear Overhauser effects (NOEs) are particularly useful in identifying pairs of protons that are spatially proximate, with interproton distances in the range 2.2–3.0 Å (Bothner-By, 1979). The observation of
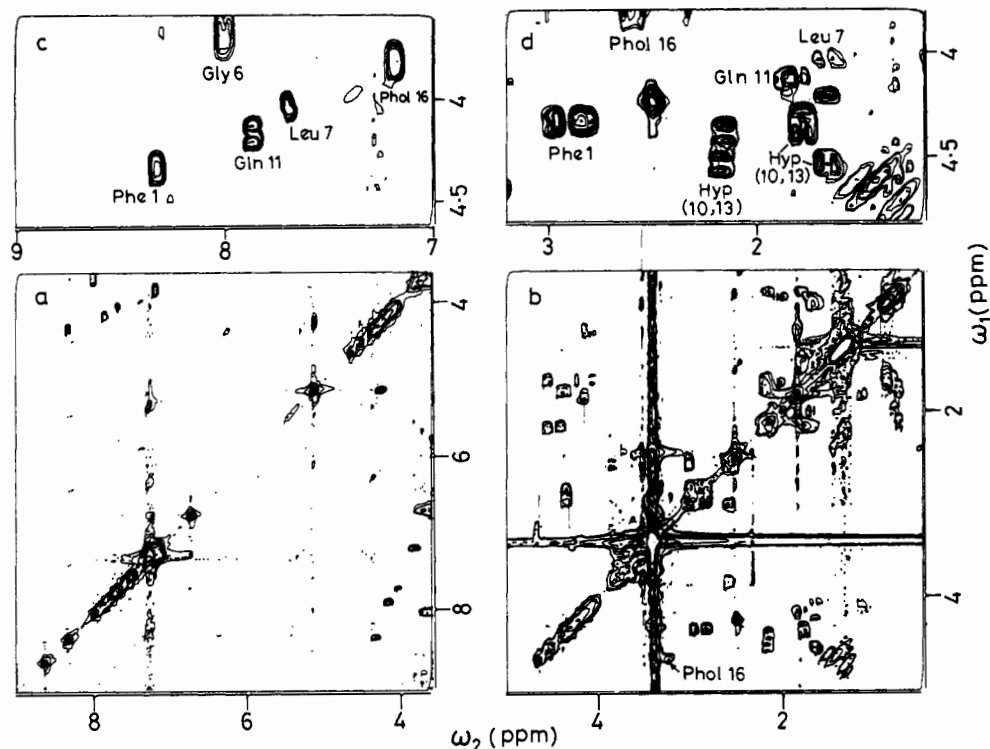
FIGURE 4: Contour plots of the COSY spectrum of antiamoebin in $(CD_3)_2SO$ (20 mg mL^{-1}): (a) δ 9.00–3.60, (b) δ 5.00–0.5, (c) expanded region of the NH–C$^\alpha$H cross peaks, and (d) expanded region of the C$^\alpha$H–C$^\beta$H cross peaks. Specific residue assignments are indicated. The Phol C$^{\beta'}$H–OH cross peak, which is crucial to identification of this residue, is marked in spectrum b. Note that the Phol C$^{\beta'}$H$_2$ protons lie very close to the water resonance.
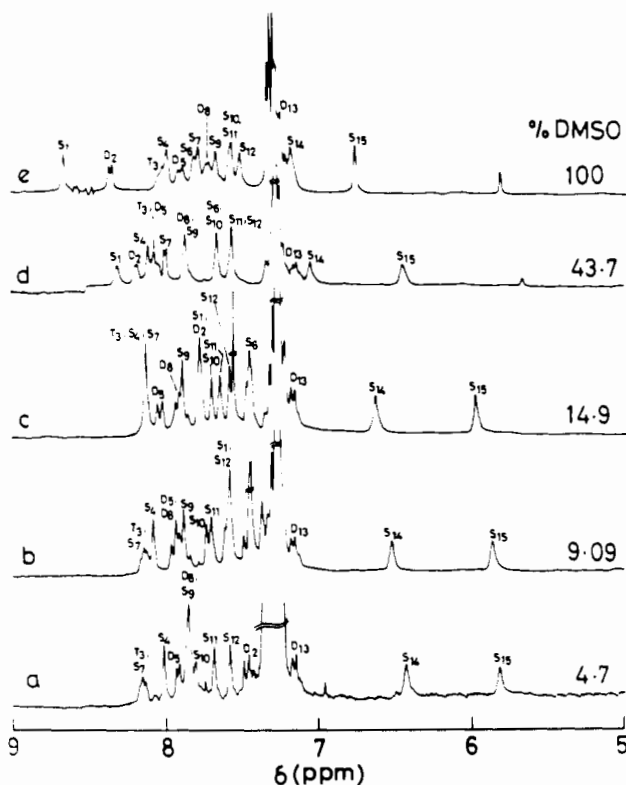

FIGURE 5: Partial 270-MHz ^{1}H NMR of antiamoebin (NH and aromatic resonances) in CDCl$_3$–$(CD_3)_2$SO mixtures. S_n, D_n, and T_n refer to singlet, doublet, and triplet NH resonances. The subscript n refers to the order of appearance from low field in $(CD_3)_2$SO.
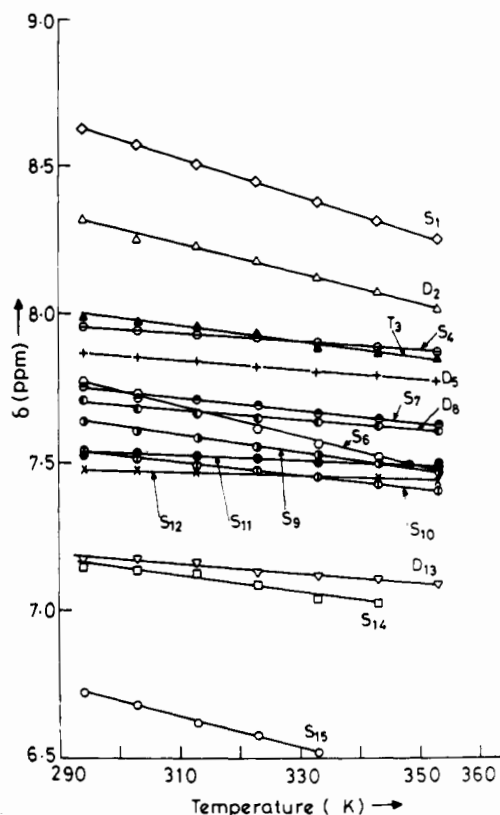

FIGURE 6: Temperature dependence of NH chemical shifts for antiamoebin in $(CD_3)_2$SO (notations as in Figure 5). Peptide concentration was 12.5 mg mL^{-1}.

interresidue NOEs (C$^\alpha_i$H–N$_{i+1}$H) in peptides is clearly diagnostic of specific peptide backbone conformations (Wüthrich et al., 1984; Shenderovich et al., 1984; Rao et al., 1983; Kishore et al., 1985; Balaram, 1985). All the NH and C$^\alpha$H

resonances of antiamoebin were individually irradiated in a systematic series of difference NOE experiments. Limited irradiation power was used to saturate resonances in order to minimize nonselective effects. Only *two* distinct *interresidue*
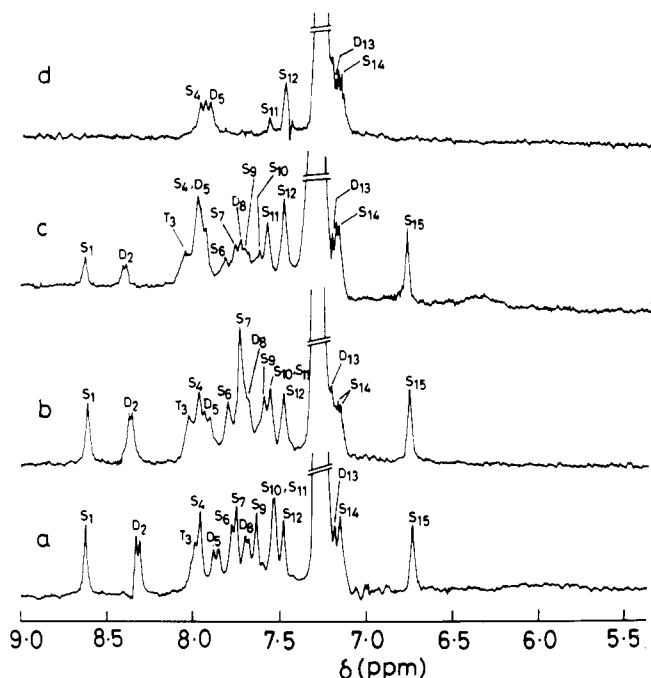
FIGURE 7: Partial 270-MHz ¹H NMR spectra in $(CD_3)_2SO$ recorded at different time intervals after addition of D_2O ($\sim 10\%$ v/v): (a) before D_2O addition and (b) 5 min, (c) 150 min, and (d) 75 h after D_2O addition. Peptide concentration was 12.5 mg mL^{-1}.
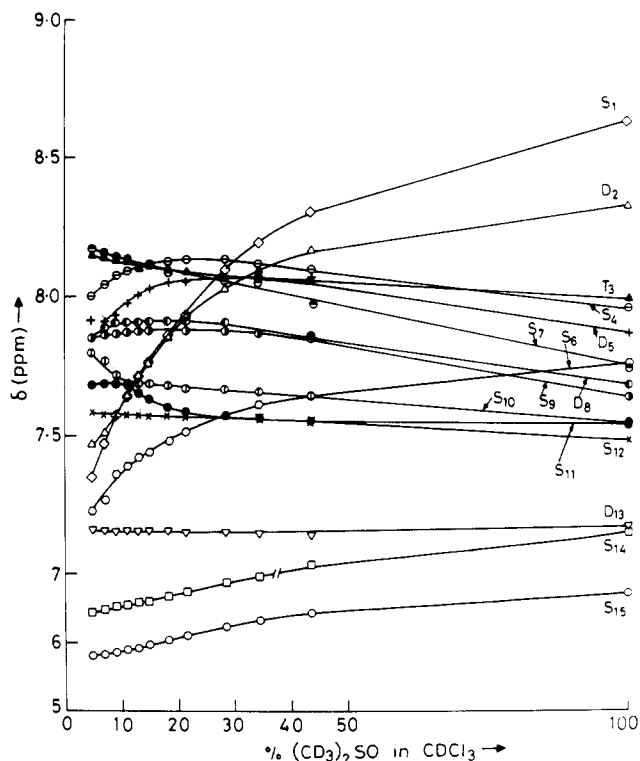

FIGURE 8: Solvent dependence of NH chemical shifts in antiamoebin as a function of $(CD_3)_2SO$ concentration in $CDCl_3$–$(CD_3)_2SO$ mixtures.

NOEs were observed, which are shown in Figure 9. A negative NOE of $\sim 10.2\%$ is observed on the Phe $C^\alpha H$ peak, when the S_1 NH resonance is saturated. Irradiation of S_6NH results in a 16.4% NOE on the Leu $C^\alpha H$ resonance. Partial saturation of closely overlapping NH resonances also occurs in this experiment. Nevertheless, the precise NOE connectivity of the S_6 NH and Leu $C^\alpha H$ resonances was readily established by systematically varying the irradiating frequency about the S_6 NH chemical shift and monitoring the magnitude of the NOE

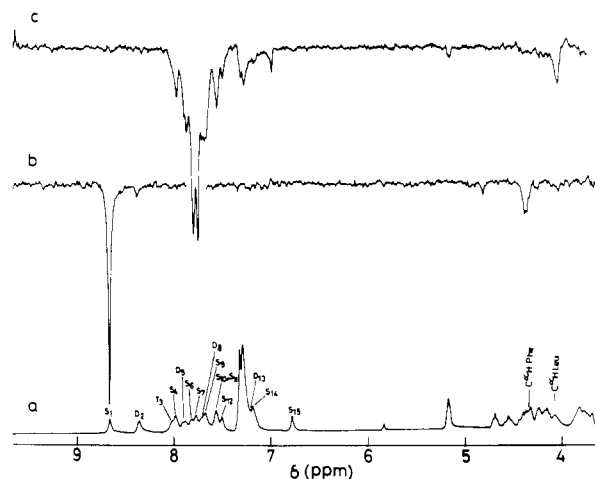FIGURE 9: (a) Partial 270-MHz ¹H NMR spectrum of antiamoebin in $(CD_3)_2SO$; (b, c) difference NOE spectra ($\times 16$) obtained by saturation of specific NH resonances, (b) Aib(2) NH and (c) Aib(8) NH. The saturated peak appears as an intense negative signal in the difference spectrum.

on the Leu $C^\alpha H$ resonance. The maximum effect is indeed observed when the irradiating frequency is centered on the S_6 NH resonance. This NOE is also clearly observed in the reverse experiment, where a decrease in intensity of 11.8% is observed for the S_6 NH resonance on saturating Leu $C^\alpha H$. These observations permit assignment of the S_1 and S_6 NH resonances to the Aib(2) and Aib(8) NH groups, respectively. It may be stressed that in peptides the only observable C^α_iH–N_jH NOEs are when $i = j$ (intraresidue) and $i + 1 = j$ (interresidue) (Wüthrich et al., 1984; Shenderovich et al., 1984).

Conformations of Antiamoebin I. The NMR results strongly suggest that antiamoebin I adopts highly folded solution conformations, in which *ten* backbone NH groups are largely inaccessible to the solvent. The formation of intramolecular $4 \rightarrow 1$ and $5 \rightarrow 1$ hydrogen bonds in Aib-containing peptides in the solid state and in solution is exceedingly well documented (Prasad & Balaram, 1984; Toniolo et al., 1983; Bosch et al., 1985a; Nagaraj & Balaram, 1981; Vijayakumar & Balaram, 1983). The solvent-shielded nature of the 10 backbone NH groups is therefore likely to be a consequence of their participation in intramolecular hydrogen bonding. The presence of several Aib/Iva residues in the antiamoebin I sequence imposes considerable stereochemical restrictions on the molecule. Aib residues are largely constrained to have conformations in the right- or left-handed $3_{10}/\alpha$-helical regions of conformational space (Prasad & Balaram, 1984), with $\phi \sim \pm 60 \pm 20°$ and $\psi \sim \pm 30 \pm 20°$ (IUPAC–IUB Commission on Biochemical Nomenclature, 1970). Similar conformational preferences have also been suggested for Iva residues from conformational energy calculations (Benedetti et al., 1984; Barone et al., 1985). The assignment of the *three* solvent exposed (non-hydrogen-bonded) NH groups to the Phe(1), Aib(2), and Aib(8) residues permits a hydrogen-bonding scheme to be proposed (Figure 10), which is fully consistent with the NMR data. The proposed scheme involves formation of *ten* $4 \rightarrow 1$ (C_{10}) hydrogen bonds. The involvement of the Phol NH group in an intramolecular hydrogen bond and its presence as the C-terminal residue in the -Iva-Hyp-Aib-Pro-Phol sequence is consistent with both $4 \rightarrow 1$ and $5 \rightarrow 1$ hydrogen-bonding possibilities. This alternative is also considered in Figure 10. Such structures have been suggested earlier for oligopeptides having a Pro residue in the center of a helical segment (Rao et al., 1980). The formation of mixed $4 \rightarrow 1$ and $5 \rightarrow 1$ hydrogen bonds, with bifurcation involving interaction
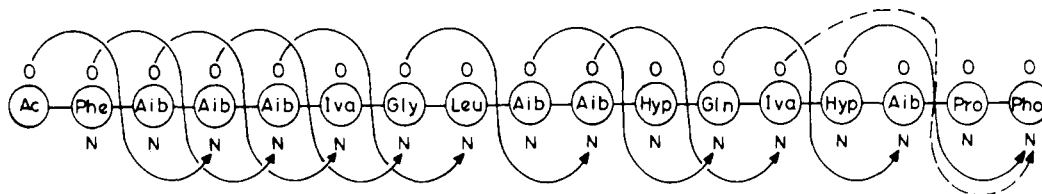
FIGURE 10: Proposed intramolecular hydrogen-bonding scheme in antiamoebin, consistent with NMR data. Arrowheads indicate hydrogen-bonded NH groups.

of a single CO group, with more than 1 NH group can also rationalize the experimental observations. Both 4→1 and 5→1 hydrogen-bonded helical structures have been observed for relatively long Aib-containing peptides in the solid state.

While the 10-residue peptide Boc-Aib-Pro-Val-Aib-Val-Ala-Aib-Ala-Aib-Aib-OMe adopts a 3_{10}-helical (4→1 hydrogen-bonded) conformation in the crystal (Francis et al., 1983), α-helical structures (5→1 hydrogen bonded) have been observed in the peptides Boc-Ala-(Aib-Ala)$_2$-Glu(OBzl)-Ala-(Aib-Ala)$_2$-OMe (Bosch et al., 1985b; Butters et al., 1981) and Boc-Trp-Ile-Ala-Aib-Ile-Val-Aib-Leu-Aib-Pro-OMe (I. L. Karle, personal communication). A mixed 4→1 and 5→1 hydrogen-bonding pattern is observed in Boc-Leu-Aib-Pro-Val-Aib-Aib-Glu(OBzl)-Gln-Phol (Bosch et al., 1985a), whereas a largely α-helical conformation has been determined for alamethicin in crystals (Fox & Richards, 1982). Homooligopeptides of Aib (Shamala et al., 1978; Benedetti et al., 1982, 1985) and Aib-X repeating sequences (Francis et al., 1985) have been shown to adopt 3_{10}-helical structures. Interestingly, the octapeptide pBrBz-(Aib)$_3$-Val-Gly-Leu-(Aib)$_2$-OMe adopts a right-handed 3_{10}-helical conformation in the solid state (Toniolo et al., 1985). This peptide corresponds to the 2–9 segment of emerimicins III and IV and has striking homology to the same segment in antiamoebin I, with only a single replacement at position 5 (Val for Iva). These observations provide some basis for the proposed hydrogen-bonding scheme in antiamoebin I (Figure 10).

The detection of only two interresidue $C^\alpha H-N_{i+1}H$ NOEs, between, viz., Phe(1) $C^\alpha H \leftrightarrow$ Aib(2) NH and Leu(7) $C^\alpha H \leftrightarrow$ Aib(8) NH, further limits the backbone conformational possibilities. Such interresidue NOEs are diagnostic of ψ_i values of ~120 ± 30°, which result in $C^\alpha_i H-N_{i+1}H$ distances of ≤2.5 Å (Shenderovich et al., 1984). Thus both Phe(1) and Leu(7) may be assigned ψ values in this region. The involvement of Aib(3) NH in an intramolecular hydrogen bond together with the observation of an NOE between Phe(1) $C^\alpha H$ and Aib(2) NH suggests the presence of a type II β-turn at the amino terminal (Rao et al., 1983; Rose et al., 1985). Such a feature would ideally have the following conformational angles at Phe(1) and Aib(2): $\phi_{Phe(1)} \sim -60°$, $\psi_{Phe(1)} \sim 120°$, $\phi_{Aib(2)} \sim 80°$, and $\psi_{Aib(2)} \sim 0°$. The continuation of the 4→1 hydrogen-bonding pattern in the amino-terminal segment requires that the succeeding β-turns fall into the type III' category ($\phi_{i+1} \approx \phi_{i+2} \approx 60°$, $\psi_{i+1} \approx \psi_{i+2} \approx 30°$). This is necessitated by the fact that Aib(2) has to simultaneously serve as the $i + 2$ residue of a type II β-turn and the $i + 1$ residue of a succeeding β-turn. The 2–6 segment of antiamoebin I thus favors a left-handed 3_{10}-helical conformation. Type II–III'–III' consecutive β-turn structures have been observed in the crystal structures of the oligopeptides p-(chlorobenzoyl)-Pro-Aib-Ala-Aib-Ala-OMe (Cameron et al., 1982) and Boc-Pro-Aib-Ala-Aib-Ala-OH (Bosch et al., 1985c).

The solvent-shielded nature of the Aib(9) NH group suggests its involvement in an intramolecular hydrogen bond. Together with the observed NOE between Leu(7) $C^\alpha H$ and Aib(8) NH protons, this supports a type II β-turn confor-

Table III: Idealized Backbone Conformational Angles for Antiamoebin I[a]

residue	ϕ (deg)	ψ (deg)	residue	ϕ (deg)	ψ (deg)
Phe(1)	−60	120	Aib(9)	−60	−30
Aib(2)	70	20	Hyp(10)	−60	−30
Aib(3)	60	30	Gln(11)	−60	−30
Aib(4)	60	30	Iva(12)	−60 (60)	−30 (30)
Iva(5)	60	30	Hyp(13)	−60 (−60)	−30 (70)
Gly(6)	60	30	Aib(14)	−60	−30
Leu(7)	−60	120	Pro(15)	−60	−30
Aib(8)	70	20	Phol(16)	−60	

[a] Structures I and II in Figure 11 are generated using these ϕ and ψ values and assuming standard geometries at the C^α atom and the peptide units. Values in parentheses for residues 12 and 13 correspond to structure II.

mation at the Leu(7)–Aib(8) segment.

While the NMR results suggest that the C-terminal NH groups, Gln(11), Iva(12), Aib(14), and Phol(16), are all hydrogen bonded, the precise conformation of the 10–16 segment is unclear. The presence of the imino acids L-Hyp and L-Pro at positions 10, 13, and 15 necessarily restricts ϕ values to ~−60 ± 15° at these residues. However, the lack of an amide hydrogen at these positions also interrupts regular helical hydrogen-bonding schemes. There are no crystal structures of large oligopeptides with such a distribution of imino acids. Theoretical studies of (Aib-Pro)$_n$ sequences have suggested that Pro residues can be incorporated into 3_{10}-helical structures with some distortions (Prasad & Balaram, 1982). Some evidence for regular helical conformations in an octapeptide with the sequence -(Aib-Pro)$_4$- has been reported (Venkatachalapathi & Balaram, 1981). In these studies C_7 (3→1 hydrogen-bonded) structures at Pro have also been considered.

In order to evaluate the influence of C-terminal conformational variations on the overall shape of antiamoebin I, ideal structures compatible with the NMR data were computer generated. Two structures were considered that differ only at Iva(12) and Hyp(13). In conformer I a fully right-handed C-terminal 3_{10}-helical segment is considered, while in conformer II a C_7 structure is used at Hyp(13) and a left-handed 3_{10}-helical conformation at Iva(12), to avoid poor intramolecular contacts. The backbone dihedral angles used are listed in Table III. Figure 11 shows a perspective view of the backbone conformations I and II. The two structures are distinctly different in overall shape, with I appearing particularly suitable for functioning as a membrane-spanning helical polypeptide. It is of interest to note that antiamoebin shows highly solvent-dependent CD spectra, suggesting a high degree of conformational variability (unpublished results). CD spectra distinct from those reported for the natural Aib-containing helical peptides, like alamethicin and suzukacillin, have been observed for antiamoebin (Brückner et al., 1984). Attempts to crystallize HPLC-purified antiamoebin I are presently in progress, in order to establish the conformation in the solid state.

Mitochondrial Uncoupling Activity. The proposed antiamoebin conformations consist of a helical amino-terminal
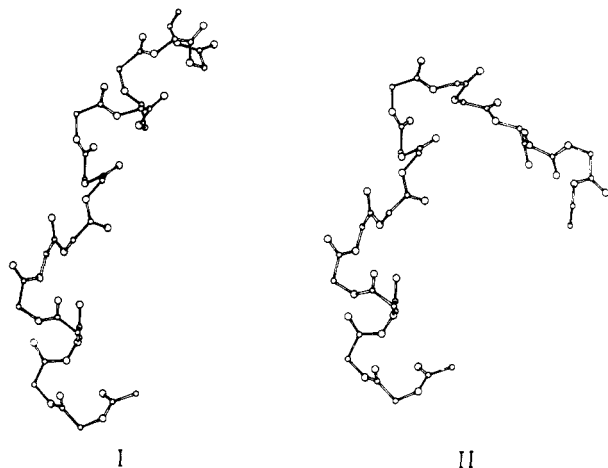
I   II

FIGURE 11: Perspective view of suggested backbone conformations I and II of antiamoebin consistent with NMR data and stereochemical constraints. Only backbone atoms are shown. Structures were generated with idealized residue geometries and the conformational angles listed in Table II. All peptide units are fixed in the trans (ω = 180°) geometry.
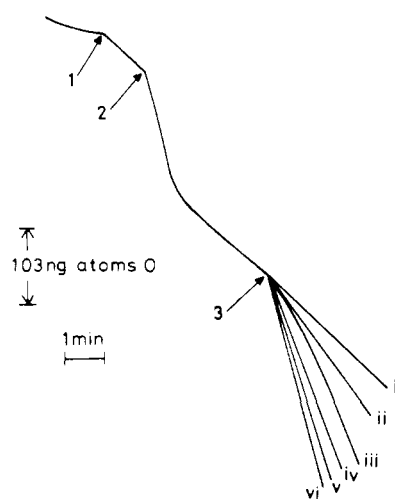

FIGURE 12: Effect of antiamoebin on state 4 respiration in rat liver mitochondria. Peptide concentrations are (i) 0.15, (ii) 0.30, (iii) 0.45, (iv) 0.60, (v) 0.75 and (vi) 0.90–1.20 μM. The mitochondria were suspended in 2 mL of 2 mM HEPES containing D-(−)-mannitol (220 mM), sucrose (70 mM), EGTA (0.5 mM), MgCl$_2$ (2.5 mM), and KH$_2$PO$_4$ (2.5 mM), pH 7.4. Points 1, 2, and 3 indicate additions of succinate (7.5 mM), ADP (72 μM), and antiamoebin, respectively. The peptide solutions were prepared in ethanol and added volumes did not exceed 9 μL. Mitochondrial concentration in the assay mixture was 0.37 mg of protein mL^{-1}.

nonapeptide, with subtle variations in handedness, and a C-terminal heptapeptide that is highly structured but not necessarily an ideal helix. Membrane channel forming activities have been rationalized with largely helical conformations, over the whole polypeptide chain, for alamethicin (Mathew & Balaram, 1983b; Boheim et al., 1983; Fox & Richards, 1982) although alternative structures have been suggested (Hall et al., 1984). In order to determine whether antiamoebin possesses membrane-modifying activities similar to alamethicin, we have examined the effect of the peptide on mitochondrial oxidative phosphorylation (Mathew et al., 1981, 1982). Figure 12 establishes that addition of antiamoebin to state 4 mitochondria results in uncoupling, at relatively low peptide concentrations. A $\phi_{1/2}$ value (concentration for half-maximal activity per milligram of mitochondrial protein) of ~0.94 nmol is estimated. This is somewhat larger than the value of ~0.16 nmol determined for natural alamethicin (M. K. Das, un-

published results). Channel formation, followed by dissipation of H$^+$ and ionic gradients across the inner mitochondrial membrane, could result in the observed uncoupling (Mathew et al., 1981). However, a general membrane-perturbing effect accompanied by enhanced ionic permeability cannot be ruled out. In the case of alamethicin, a transition from uncoupling to inhibitory activity has been observed, with increasing concentration of phosphate in the assay medium. This has been attributed to the transport of phosphate ions through alamethicin channels (Das et al., 1985). Antiamoebin behaves purely as an uncoupler over the phosphate concentration range 2.5–100 mM. It remains to be established whether differences in membrane-modifying activities of alamethicin and antiamoebin can be correlated to secondary structure differences. Antiamoebin has also been shown to induce Ca^{2+} flux across liposomal membranes (M. K. Das, unpublished results), suggesting that peptide incorporation can indeed result in cation transport across lipid bilayers.

REFERENCES

Aue, W. P., Bartholdi, E., & Ernst, R. (1976) J. Chem. Phys. 64, 2229–2246.
Balaram, P. (1985) Proc. Indian Acad. Sci., Chem. Sci. 95, 21–38.
Balasubramanian, T. M., Kendrick, N. C. E., Taylor, M., Marshall, G. R., Hall, J. E., Vodyanoy, I., & Reusser, F. (1981) J. Am. Chem. Soc. 103, 6127–6132.
Banerjee, U., Tsui, F. P., Balasubramanian, T. M., Marshall, G. R., & Chan, S. I. (1983) J. Mol. Biol. 165, 757–775.
Barone, V., Lelj, F., Bavoso, A., DiBlasio, B., Grimaldi, P., Pavone, V., & Pedone, C. (1985) Biopolymers 24, 1759–1767.
Benedetti, E., Bavoso, A., DiBlasio, B., Pavone, V., Pedone, C., Crisma, M., Bonora, G. M., & Toniolo, C. (1982) J. Am. Chem. Soc. 104, 2437–2444.
Benedetti, E., Toniolo, C., Hardy, P., Barone, V., Bavoso, A., DiBlasio, B., Grimaldi, P., Lelj, F., Pavone, V., Pedone, C., Bonora, G. M., & Lingham, I. (1984) J. Am. Chem. Soc. 106, 8146–8152.
Benedetti, E., DiBlasio, B., Pavone, V., Pedone, C., Bavoso, A., Toniolo, C., Bonora, G. M., Leplawy, M. T., & Hardy, P. M. (1985) J. Biosci. 8, 253–262.
Bodo, B., Rebuffat, S., El Hajji, M., & Davoust, D. (1985) J. Am. Chem. Soc. 107, 6011–6017.
Boheim, G., & Kolb, H. A. (1978) J. Membr. Biol. 38, 99–150.
Boheim, G., Janko, K., Leibfritz, D., Ooka, T., Konig, W. A., & Jung, G. (1976) Biochim. Biophys. Acta 433, 182–199.
Boheim, G., Irmscher, G., & Jung, G. (1978) Biochim. Biophys. Acta 507, 485–506.
Boheim, G., Hanke, W., & Jung, G. (1983) Biophys. Struct. Mech. 9, 181–191.
Bosch, R., Jung, G., Schmitt, H., & Winter, W. (1985a) Biopolymers 24, 979–999.
Bosch, R., Jung, G., Schmitt, H., & Winter, W. (1985b) Biopolymers 24, 961–978.

Bosch, R., Jung, G., Schmitt, H., & Winter, W. (1985c) *Acta Crystallogr., Sect. C: Cryst. Struct. Commun. C41*, 1821–1825.

Bothner-By, A. A. (1979) in *Magnetic Resonance in Biology* (Shulman, R. G., Ed.) pp 177–219, Academic, New York.

Brückner, H., & Przybylski, M. (1984) *J. Chromatogr. 296*, 263–275.

Brückner, H., Graf, H., & Bokel, M. (1984) *Experientia 40*, 1189–1197.

Butters, T., Hutter, P., Jung, G., Pauls, N., Schmitt, H., Sheldrick, G. M., & Winter, W. (1981) *Angew. Chem., Int. Ed. Engl. 20*, 889–890.

Cameron, T. S., Hanson, A. W., & Taylor, A. (1982) *Cryst. Struct. Commun. 11*, 321–330.

Das, M. K., Basu, A., & Balaram, P. (1985) *Biochem. Int. 11*, 357–363.

Davoust, D., Bodo, B., Rebuffat, S., & Platzer, N. (1983) *Biochem. Biophys. Res. Commun. 116*, 1–8.

Fox, R. O., & Richards, F. M. (1982) *Nature (London) 300*, 325–330.

Francis, A. K., Iqbal, M., Balaram, P., & Vijayan, M. (1983) *FEBS Lett. 155*, 230–232.

Francis, A. K., Vijayakumar, E. K. S., Balaram, P., & Vijayan, M. (1985) *Int. J. Pept. Protein Res. 26*, 214–223.

Fujita, T., Takaishi, Y., Matsuura, K., Takeda, Y., Yoshioka, Y., & Bruckner, H. (1984) *Chem. Pharm. Bull. 32*, 2870–2873.

Hall, J. E., Vodyanoy, I., Balasubramanian, T. M., & Marshall, G. R. (1984) *Biophys. J. 45*, 233–247.

IUPAC-IUB Commission on Biochemical Nomenclature (1970) *Biochemistry 9*, 3471–3479.

Jung, G., Bruckner, H., & Schmitt, H. (1981) in *Structure and Activity of Natural Peptides* (Voelter, W., & Weitzel, G., Eds.) pp 75–114, Walter de Gruyter, Berlin.

Katz, E., Aydin, M., Lucht, N., Konig, W. A., Ooka, T., & Jung, G. (1985) *Liebigs Ann. Chem.* 1041–1062.

Kessler, H. (1982) *Angew. Chem., Int. Ed. Engl. 21*, 512–523.

Kishore, R., Kumar, A., & Balaram, P. (1985) *J. Am. Chem. Soc. 107*, 8019–8023.

Martin, D. R., & Williams, R. J. P. (1976) *Biochem. J. 153*, 181–190.

Mathew, M. K., & Balaram, P. (1983a) *Mol. Cell. Biochem. 50*, 47–64.

Mathew, M. K., & Balaram, P. (1983b) *FEBS Lett. 157*, 1–6.

Mathew, M. K., Nagaraj, R., & Balaram, P. (1981) *Biochem. Biophys. Res. Commun. 98*, 548–555.

Mathew, M. K., Nagaraj, R., & Balaram, P. (1982) *J. Biol. Chem. 257*, 2170–2176.

Mueller, P., & Rudin, D. O. (1967) *Nature (London) 217*, 713–719.

Nagaraj, R., & Balaram, P. (1981) *Acc. Chem. Res. 14*, 356–362.

Nagayama, K., & Wüthrich, K. (1981) *Eur. J. Biochem. 114*, 356–374.

Pandey, R. C., Carter Cook, J., Jr., & Rinehart, K. L., Jr. (1977a) *J. Am. Chem. Soc. 99*, 8469–8483.

Pandey, R. C., Carter Cook, J., Jr., & Rinehart, K. L., Jr. (1977b) *J. Am. Chem. Soc. 99*, 5205–5206.

Pandey, R. C., Meng, H., Carter Cook, J., Jr., & Rinehart, K. L., Jr. (1977c) *J. Am. Chem. Soc. 99*, 5203–5205.

Pandey, R. C., Carter Cook, J., Jr., & Rinehart, K. L., Jr. (1978) *J. Antibiot. 31*, 241–242.

Prasad, B. V. V., & Balaram, P. (1982) *Int. J. Biol. Macromol. 4*, 99–102.

Prasad, B. V. V., & Balaram, P. (1984) *CRC Crit. Rev. Biochem. 16*, 307–348.

Przybylski, M., Dietrich, I., Manz, I., & Brückner, H. (1984) *Biomed. Mass Spectrom. 11*, 569–582.

Rao, B. N. N., Kumar, A., Balaram, H., Ravi, A., & Balaram, P. (1983) *J. Am. Chem. Soc. 105*, 7423–7428.

Rao, C. P., Nagaraj, R., Rao, C. N. R., & Balaram, P. (1980) *Biochemistry 19*, 425–431.

Rinehart, K. L., Jr., Pandey, R. C., Moore, M. L., Tarbox, S. R., Snelling, C. R., Carter Cook, J. C., Jr., & Milberg, R. H. (1979) in *Peptides: Structure and Biological Function* (Gross, E., & Meienhofer, J., Eds.) pp 59–71, Pierce Chemical, Rockford, IL.

Rinehart, K. L., Jr., Gaudioso, L. A., Moore, M. L., Pandey, R. C., Carter Cook, J., Jr., Barber, M., Sedgwick, R. D., Bordoli, R. S., Tyler, A. N., & Green, B. N. (1981) *J. Am. Chem. Soc. 103*, 6517–6520.

Rose, G. D., Gierasch, L. M., & Smith, J. A. (1985) *Adv. Protein Chem. 37*, 1–109.

Shamala, N., Nagaraj, R., & Balaram, P. (1978) *J. Chem. Soc., Chem. Commun.*, 996–997.

Shenderovich, M. D., Nikiforovich, G. V., & Chipens, G. I. (1984) *J. Magn. Reson. 59*, 1–12.

Stroh, J. G., Carter Cook, J. C., Jr., Milberg, R. M., Brayton, L., Kihara, T., Huang, Z., Rinehart, K. L., Jr., & Lewis, I. A. S. (1985) *Anal. Chem. 57*, 985–991.

Thirumalachar, M. J. (1968) *Hind. Antibiot. Bull. 10*, 287–289.

Toniolo, C., Bonora, G. M., Bavoso, A., Benedetti, E., DiBlasio, B., Pavone, V., & Pedone, C. (1983) *Biopolymers 22*, 205–215.

Toniolo, C., Bonora, G. M., Bavoso, A., Benedetti, E., DiBlasio, B., Pavone, V., & Pedone, C. (1985) *J. Biomol. Struct. Dyn. 3*, 585–598.

Venkatachalapathi, Y. V., & Balaram, P. (1981) *Biopolymers 20*, 1137–1145.

Vijayakumar, E. K. S., & Balaram, P. (1983) *Biopolymers 22*, 2133–2140.

Wider, G., Macura, S., Kumar, A., Ernst, R. R., & Wüthrich, K. (1984) *J. Magn. Reson. 56*, 207–234.

Wüthrich, K. (1976) *NMR in Biological Research: Peptides and Proteins*, North-Holland, Amsterdam.

Wüthrich, K., Billeter, M., & Braun, W. (1984) *J. Mol. Biol. 180*, 715–740.